Translational Energy Effects in the $Ca^*(^1D_2) + HBr \rightarrow CaBr^*(A,B)$ Reaction. Experimental Evidence of Synchronization between Electron Transfer and Rearrangement of the Intermediate Complex

Miguel De Castro, Roberto Candori, Fernando Pirani, Vincenzo Aquilanti, Macarena Garay,* and Angel González Ureña*,†

Dipartimento di Chimica, Università di Perugia I-06123 Perugia, Italy, and Unidad de Laseres y Haces Moleculares, Instituto Pluridisciplinar—Universidad Complutense de Madrid, 28040 Madrid, Spain

Received: May 1, 1998; In Final Form: July 8, 1998

The collision energy dependence of the $Ca^*(^1D_2) + HBr \rightarrow CaBr^*(A,B) + H$ reaction cross sections has been measured over the 210−290 meV range using the time-of-flight technique under crossed molecular beam conditions. Both reaction channels show a steep increase with pronounced maximum at low energy, followed by a sharp decline as energy increases. A modified time-dependent Landau−Zener model is employed to describe the transition probability from the entrance neutral to the exit ionic channels, directly leading to reaction products. This model, which incorporates the influence on the reaction dynamics of the time necessary for the rearrangement of the intermediate complex, satisfactorily accounts for the experimentally observed translational features of the excitation functions.

1. Introduction

The reactions involving excited calcium atoms and hydrogen halides molecules, to give chemiluminescent products, were first studied by Telle et al.[1] through beam-gas experiments. The high value of measured cross sections suggested that a "harpooning" type mechanism, involving an electron jump, is controlling the reaction dynamics. Subsequently, this type of reactions has been the object of considerable experimental attention using either scattering studies, leading to measurement of alignment effects both in the reagents and in the products,[2,3] or laser excitation of van der Waals Ca−HX complexes, which have a configuration close to that of the reaction transition state.[4] However, because no accurate potential energy surfaces are presently available, energy and positions of crossings and couplings between the entrance (neutral) and exit (ionic) potential energy surfaces are unknown and the details of reaction dynamics remain to be understood.

In the present paper we report on a crossed-beam study of the $Ca^*(^1D_2) + HBr \rightarrow CaBr^*(A,B) + H$ reactions using the time-of-flight technique described elsewhere.[5] This high-resolution, full-collision technique provides a direct means to measure, for both channels, the collision energy dependence of the chemiluminescent reaction cross sections. Present scattering data reveal that both the investigated reactions exhibit excitation functions with a steep rise at low energy, and a pronounced maximum at intermediate values (≃215 meV) followed by a sharp decrease at higher energies. These features cannot be represented within a typical Landau−Zener treatment, usually employed to describe nonadiabatic processes in systems involving atoms or monatomic ions, mainly because of the sharp falloff observed at energies higher than those of the maximum.

An empirical estimate of the interaction in specific geometries of the collision complex, particularly taking into account for the anisotropy due to the Ca* orbital alignment and to the HBr molecular orientation, allows the characterization of the sequence of elementary events which occur at crossings between potential energy surfaces. In addition, because the reaction is triggered by an electron transfer from the Ca* to HBr and proceeds via a molecular rearrangement within the $Ca^+\cdots HBr^-$ complex, the nonadiabatic transition from the entrance neutral to the exit ionic channels, directly leading to products, must follow some synchronization requirement. In fact, the electron transfer is an essentially instantaneous event compared with the molecular rearrangement, which occurs in the time scale of bending and stretching motions. A lower limiting value for the range of impact parameters, which can lead to reaction is obtained by the requirement that the time associated with a nonadiabatic transition, as calculated according to the formula proposed by Bobashev and Kharchenko,[6] must be comparable to or longer than the time necessary for molecular rearrangement. As stressed in the following, both these two aspects, namely, the evaluation of the anisotropic interaction in the entrance channels and the impact parameters limitation due to the time restriction, are relevant to account for the observed behavior.

The present study is focused on the global energy dependence of the excitation function measured for both CaBr* (A,B) products. A full analysis which takes into account fine details of the reactive cross sections, such as stair-like behaviors observed for the Ca* + HX (X = Cl, Br) reactions,[7] will be presented in a future paper.

2. Experimental Apparatus and Results

The experimental apparatus couples the crossed-beam technique with the measurement in coincidence of the chemiluminescence yield of products. Because the main features of the experimental setup are well described elsewhere,[5] only basic details are reported here. As shown schematically in Figure 1 a pulsed beam of electronically excited Ca* atoms in their $^1D_2$ state, formed though a pulsed discharge in an oven source, undergoes collisions with a cooled, continuous and seeded

* To whom correspondence should be addressed.
† Unidad de Laseres y Haces Moleculares.

10.1021/jp982085k CCC: $15.00
Published on Web 09/17/1998

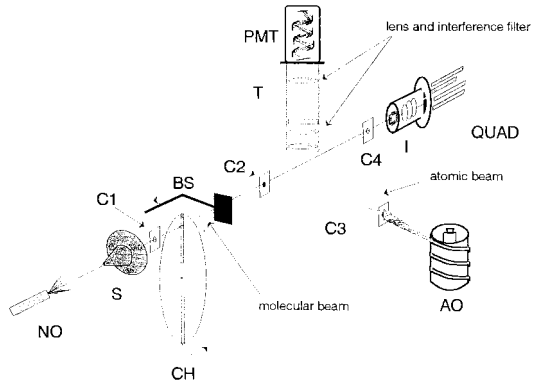

Figure 1. Schematic view of the experimental setup. NO, nozzle oven; AO, atomic oven; S, skimmer; CH, chopper; C1, C2, C3, and C4, collimators; BS, beam stop; PMT, photomultiplier; QUAD, quadrupole mass filter.

TABLE 1: Experimental Conditions

HBr beam velocity (m s^{-1})	1.2×10^3
Ca oven temperature (K)	1400
pulse discharge voltage (V)	35−50
pulse discharge current (A)	0.8
Ca flight path (cm)	11
collision energy resolution (meV)	15−20

TABLE 2: Ca + HBr → CaBr + H Reaction Energetics

reaction	ΔH_0^0 (meV)
$Ca(^1S_0) + HBr \rightarrow CaBr(X^2\Sigma^+) + H$	258.1
$Ca^*(^3P_J) + HBr \rightarrow CaBr^*(A^2\Pi) + H$	343.6
$Ca^*(^3P_J) + HBr \rightarrow CaBr^*(B^2\Sigma^+) + H$	398.0
$Ca^*(^1D_2) + HBr \rightarrow CaBr^*(A^2\Pi) + H$	−476.7
$Ca^*(^1D_2) + HBr \rightarrow CaBr^*(B^2\Sigma^+) + H$	−421.8

supersonic HBr beam. The photon counting technique is used to collect the spontaneous CaBr* fluorescence as a function of the Ca* arrival time. Thus, by using narrow interference filters, different electronic emission bands can be isolated and measured. Peak velocity of the stationary beam, and the discharge and the oven source conditions of the pulsed beam are reported in Table 1 together with other relevant experimental features. The pulsed calcium beam was produced at a repetition frequency of 2500 Hz which allows one to accomplish, for each experimental run, a good statistics in short periods of time.

A crucial point is the appropriate identification of the investigated reaction channels. The energetics, summarized in Table 2, suggests that chemiluminescence can be observed only for the CaBr* product in its A or B excited states, formed in collisions between $Ca^*(^1D_2)$ and HBr. Other channels, originating from the presence in the pulsed beam of atoms in the ^3P_J levels, are closed (see Table 2) in the collision energy range (210−290 meV) here investigated.

Essentially, the experiment consists of measuring the time profile of the CaBr* emission, $I_{CaBr}(t)$, as a function of the time arrival of the beam of the metastable $Ca^*(^1D_2)$, of density $N_{Ca}(t)$. The most significant features of the experimental technique are (a) direct access to obtain the collision energy dependence of the reaction cross-section $\sigma(E)$ [indeed, a simple estimation of the ratio of the two above-mentioned observable, e.g., $I_{CaBr}(t)/N_{Ca}(t)$ leads to $\sigma(E)$ (see below)] and (b) a high resolution in the collision energy. The latter is the result of three factors: (i) a narrow HBr beam velocity distribution with a full width half-maximum (fwhm), of the order of 4%; (ii) short pulses used in the production of the metastable $Ca^*(^1D_2)$ atoms; (iii) a high resolution in the data acquisition, based on the use of fast response photomultiplier and photon counting techniques.

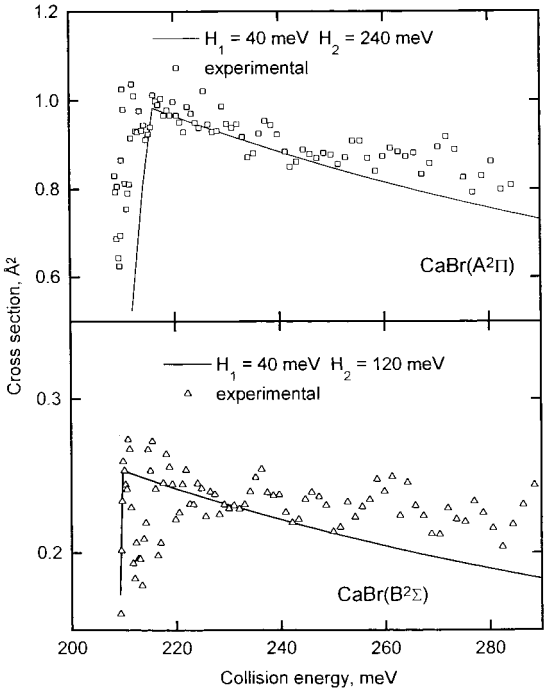

Figure 2. Collision energy dependence of the reaction cross section for the two chemiluminescent $Ca^*(^1D_2) + HBr \rightarrow CaBr^*$ (A,B) + H reactions as indicated. Open symbols: experimental data in arbitrary units. Solid line: calculated using the dynamical treatment illustrated in the text.

Altogether, when a few (2−4) microseconds pulse is used, an energy resolution of typically 20 meV, at a collision energy of ≃210 meV, can be achieved.

For a given average relative velocity $v(t)$, to which corresponds the average collision energy E, the reaction cross section $\sigma(E)$ can be obtained from measurements of $I_{CaBr}(t)$ and $N_{Ca}(t)$ via the relationship:[5]

$$\sigma(E) = \frac{I_{CaBr}(t)}{N_{Ca}(t) N_{HBr} v(t) \Delta V} \qquad (1)$$

where ΔV is the collision volume and N_{HBr} the HBr beam density. Because N_{HBr} and ΔV are constant during an experiment, relative values of the reaction cross-section can be obtained from the experimental $I_{CaBr}(t)/N_{Ca}(t)$ ratio and $v(t)$. Figure 2 shows the excitation function for $CaBr^*(B,^2\Sigma^+)$ and $CaBr^*(A,^2\Pi)$ chemiluminescence channels. Both excitation functions show a steep increase with a pronounced maximum at low energy (≃215 meV), followed by a sharp decline as the collision energy increases. Notice that although all experimental conditions were identical, some bumps are more noticeable for the $CaBr^*(B,^2\Sigma^+)$ reaction channel than for the other one.

3. Nature of the Interactions and Their Modeling

Similarly to the previously considered case of the analogous reactions involving HCl,[8] the main process leading to reaction is dominated by a harpooning mechanism (i.e., a charge exchange phenomenon taking place at crossings between covalent and ionic surfaces) combined with molecular rearrangement which finally opens up the exit channels to products.

An accurate picture of such surfaces, as needed to describe these crossings, requires consideration of the combined effect of three interaction terms of different nature: (i) an anisotropic *van der Waals component*, between neutral partners having non spherical charge distribution; (ii) an *electrostatic potential*

involving permanent dipolar and quadrupolar terms; and (iii) a term accounting for *charge-transfer effects*.

The *van der Waals component* is due to a critical balancing between a long-range dispersion attraction, originated by induced multipole attraction, and a short-range repulsion, associated to the size of the outer electronic orbitals.[9] Both attraction and repulsion, which vary with the relative orientation of the Ca* atomic orbital and the HBr molecular bond, can be accurately represented in terms of the anisotropic atomic and molecular polarizabilities.[8,10]

The *electrostatic potential* originates from the interaction between the permanent dipole and quadrupole on HBr molecule with the permanent quadrupole on the Ca* atom.[11] This is another anisotropic contribution to the potential energy which vanishes upon averaging over orientations, even considering only one of the two partners.

Charge-transfer effects take place between the outer valence electron orbitals of the Ca* atom and the unoccupied antibonding orbital of the HBr molecule, mainly localized on the H atom. As is well-known, the effectiveness of this contribution basically depends on the orbital overlap which strongly varies with the intermolecular distance.[12] The relative role of the (i) and (iii) components and the proper evaluation of the potential parameters have been recently discussed[10] in order to describe the energetics of the bonding in the Ca···HX complexes in the ground electronic state.

In the previous paper on the Ca* + HCl reaction,[8] the orientational effects of HCl molecule were considered as negligible when compared with those coming from the alignment of the atomic orbital in the entrance channel of the collision, and an overall description of the harpooning mechanism was presented. A full understanding of the collisional dynamics requires the inclusion of the effect of the molecular orientation which is mainly due to anisotropic electrostatic forces. Because electrostatic effects provide the largest contribution in the collinear geometry with the hydrogen atom in the intermediate position,[11] and they play a minor role when the molecular bond is orthogonal to the intermolecular axis, an appreciable modification of the interaction picture, as previously given in ref 8, will have to be considered only for the collinear geometry. It is also appropriate to note here that a similar approach should also account for some fine structures measured for the Ca* + HCl reaction and not explicitly analyzed previously.[8]

Figure 3 reports cuts in the perpendicular geometry of potential energy surfaces in the entrance channel that asymptotically belong to Π symmetry, the label applying at distances so large that the HBr can be taken as a spherical particle. They correlate with Ca* ($^1P_1$) and Ca* ($^1D_2$) excited atomic levels. These cuts are those mainly responsible, as discussed below, for the formation of CaBr*(A,B), and have been defined and parametrized according to the same procedure illustrated in ref 8, where the interaction potential is given in terms of a spherical component (V_0 term) of van der Waals nature, plus an anisotropic term (V_2), which includes both charge transfer and atomic alignment effects. The V_0 potential is represented by a Morse function (see ref 8) with curvature parameter $\beta = 5.0$ and well depth $\epsilon = 16.6$ meV at an equilibrium distance $R_m = 5.14$ Å. The V_2 component is described by an exponential function of distace with an exponential factor $\alpha = 1.1$ Å^{-1} and a preexponential term $C = 106500$ meV. An ionic channel, asymptotically leading to Ca^+ (^2D) + HBr^- ($^2\Sigma$), also parametrized according to ref 8, is also reported in Figure 3. The

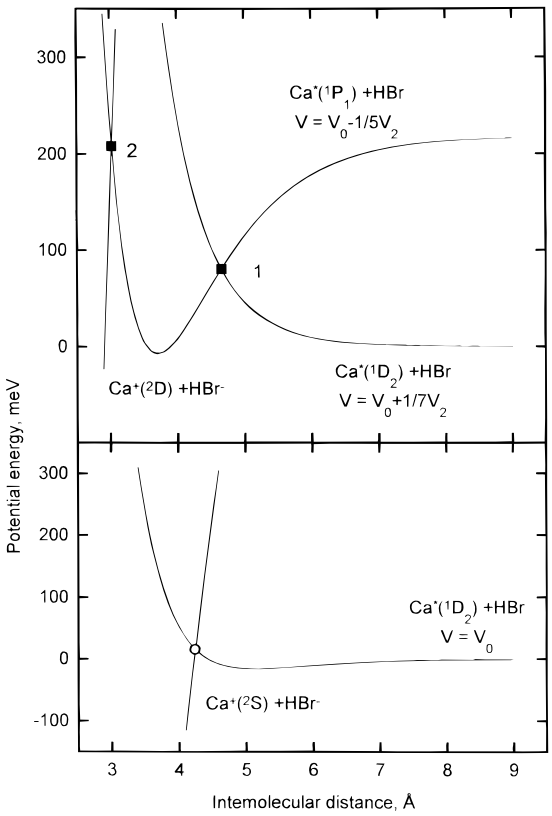

Figure 3. Cuts of the potential energy surfaces mainly responsible of the effects measured in the energy dependence of the reactive cross sections. The upper panel represent the interaction when both the Ca* 4p orbital and HBr bond approach perpendicularly with respect the intermolecular axis. This configuration leads to excited CaBr* products. The lower panel refers to the case of a collinear approach, with both the atomic 4p orbital and the HBr bond aligned along the intermolecular axis. This configuration contributes to the formation of the products in the ground electronic state. Ionic curves are also shown and the potentials are parametrized as discussed in the text and in ref 8. (Note that a misprint is present in eq 8 of ref 8. The correct definition of the interactions in terms of V_0 and V_2 are reported in the figure).

asymptotic level of this channel has been assessed attributing to HBr a vertical electron affinity corresponding to -0.4 eV.[13]

As suggested in our previous analysis,[8] the outer potential energy crossing in the entrance covalent channels (labeled as 1 in Figure 3), is believed to be responsible for the opening of the path to the inner one (labeled as 2 in Figure 3), which directly leads to reaction products in the two electronic excited states, $A^2\Pi$ and $B^2\Sigma$, responsible of the observed chemiluminescence.

The outer crossing gives rise to a mixing between states associated with different atomic levels, Ca*($^1P_1$) and Ca*($^1D_2$), also suggested by some features observed in the action spectra measured for this system.[4] The inner crossing occurs between the entrance channel Ca* ($^1P_1$) + HBr and the ionic potential. These crossings involve an electron jump from the 4s atomic orbital of Ca* to the lowest unoccupied antibonding molecular orbital of HBr, which preferentially occurs when the Ca* 4p orbital and the HBr bond are both perpendicularly aligned with respect to the intermolecular axis.

Collinear approaches of the 4p orbital and HBr molecule both aligned along the intermolecular axis, and unfavored by the van der Waals repulsion,[9] are instead stabilized by the electrostatic potential and charge transfer;[11,12] opposite anisotropic contributions generate balancing effects, so that globally the interaction turns out to be close to the spherical component V_0, and results

are shown in the lower part of Figure 3. Therefore, the electrostatic component must be here explicitly taken into account; indeed, the jump of the 4p electron makes possible the reaction in the collinear approach also, which correlates with the formation of the product CaBr in the electronic ground state (X).

Therefore the formation of the products in the ground (X) and in the excited (A,B) states originates from different angular cuts of the potential energy surfaces, which correspond to different geometries for the transition state.

The present analysis focuses on the direct formation of the CaBr*(A,B) from excited reagents approaching according to specific geometries for which the potential representation reported in the upper part of Figure 3 is appropriate.

A full treatment for the reaction dynamics, including contributions from different angles of approach on the potential energy surfaces, will be presented in a more detailed future paper, which will provide a complete description of this as well of the analogous reactions with HCl.

4. Reaction Dynamics

The dynamical treatment of the formation of CaBr* in the excited (A,B) states must proceed through the characterization of the sequence of the elementary events which take place at the crossings between potential energy surfaces. Insight into the mechanism is obtained by treating nonadiabatic events at crossings independently, and then combining them to give the total probability P of transition in each exit channel. The P value can be given in terms of a proper combination of p_x, the probability of diabatic passage though the xth curve crossing (x =1, 2 in Figure 3). For the calculation of p_x we use the classic formula of Landau, Zener, and Stückelberg:[14−16]

$$p_x(v_R,b) = \exp\left(-\frac{2\pi H_x^2}{\hbar v_R \Delta_x}\right) \tag{2}$$

where H_x is the matrix element of nonadiabatic coupling at the xth crossing, Δ_x is the absolute value of the difference between the slopes of the involved potential energy curves, and v_R is the radial velocity at the same crossing given by

$$v_R^2 = \frac{2}{\mu}\left[E\left(1-\frac{b^2}{R_x^2}\right) - E_x\right] \tag{3}$$

μ is the reduced mass of the system, E is the collision energy in the center-of-mass frame, b is the impact parameter, and E_x and R_x are energy and location of the xth crossing.

The total reactive cross section σ is obtained numerically integrating the probability P over the impact parameter b:

$$\sigma(E) = 2\pi\int_{b_0}^{b_{max}} P(E) b \, db \tag{4}$$

where

$$b_{max} = R_i\left(1-\frac{E_i}{E}\right)^{1/2} \tag{5}$$

is the maximum value of the impact parameter for which v_R of eq 3 is real.

Typically, as for atom−atom collisions, b_0 is taken equal to zero, but the following treatment will show that the need for synchronization between electron jump and molecular rearrangement will exclude small b values.

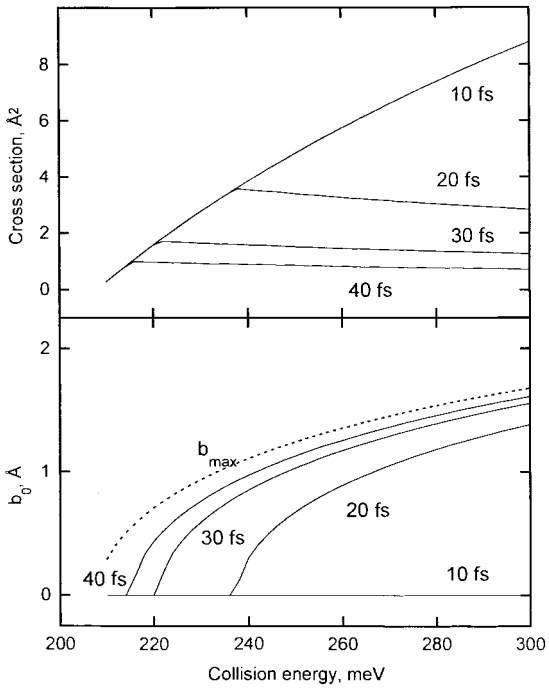

Figure 4. Upper panel: Reactive cross section σ calculated at different rearrangement times, τ_0, in femtoseconds, of the intermediate complex and as function of the averaged collision energy. Note that the typical Landau−Zener behavior appears for $\tau_0 \leq 10$ fs. Lower panel: lower limit, b_0, for the impact parameter range, to be used in eq 4, calculated according to eq 6 and 3 and at the indicated τ_0 values in femtoseconds.

As discussed before the outer crossing induces the collisional excitation to Ca*(^{1}P$_1$) from Ca*(^{1}D$_2$), while the inner one is mainly responsible for the reaction dynamics: the process starts with an electron excitation followed by an electron transfer, both assumed as being instantaneous (no time restriction), and continues with a molecular rearrangement. The latter involves bending of the complex and stretching of the HBr bond within the charge transfer complex and occurs in a time scale of the order of these motions. As a consequence the transition from the entrance neutral to the exit ionic channels, directly leading to products, requires synchronization, in the sense that only those collisions which exceed possible energy thresholds in the entrance channels and which occur in a time scale sufficiently long, to induce molecular rearrangement, will effectively cause the reaction to proceed.

Bobashev and Kharchenko[6] have proposed the following expression for the time τ associated to a nonadiabatic transition:

$$\tau = \left[\left(\frac{\hbar}{2v_R\Delta}\right)^2 + \left(\frac{H_x}{v_R\Delta}\right)^4\right]^{1/4} \tag{6}$$

The transition time τ is seen to be due to two contributions: the first is dominant when the H_x term is small and the product $v_R\Delta$ is sufficiently large: this applies to the sudden (or diabatic) limiting case. The second term is important in the opposite situation and describes the adiabatic limiting case. Both these terms depend on the radial velocity v_R and thus τ is a function of the impact parameter. This formula has been applied to the inner crossing (labeled as 2 in Figure 3) and only those nonadiabatic transitions, which have a τ value larger than the typical rearrangement time for the collision complex τ_0, have been considered as having an affect on the reaction probability. This synchronization restriction limits the effective impact parameter range to values higher than a b_0 ($b_0 \geq 0$), which provides the lower integration limit in eq 4. In Figure 4 (lower

part) we report the b_0 value, as a function of the collision energy E and for a set of different τ_0 values, as obtained from the potential interaction shown in Figure 3 and calculated combining eq 3 and 6, assuming for the coupling matrix element in the inner crossing H_2 the value 240 meV. In the same figure we also report the b_{max} value calculated according to eq 5. It is important to note that the reaction window for impact parameters (i.e., the range $b_0 - b_{max}$) increases with the collision energy when b_0 is equal to zero. In such conditions the reaction cross section follows a typical Landau−Zener behavior shown in the upper part of Figure 4. The reaction window decreases, as the energy increases, when synchronization is required, that is, when b_0 is different from zero. Then this restriction in the impact parameter range gives rise to a falloff in the energy dependence of cross sections, which appears evident, in the energy range of the present experiment, (210−290 meV), when $\tau_0 \geq 10$ fs. Furthermore the slope of the falloff is found to be nearly independent of the specific τ_0 value.

In Figure 2, calculated cross sections for the formation of the excited CaBr*(A,B) states are compared with the experimental data. Calculations have been performed assuming $\tau_0 =$ 40 fs and a coupling H_1, for outer crossing, equal to 40 meV in both cases: as seen before this crossing produces the mixing of atomic states which opens up both reaction paths. Because the formation of the A state involves a homogeneous inner crossing and the B state a heterogeneous crossing,[8] the couplings are assumed to be different: $H_2 = 240$ meV for the A state and $H_2 = 120$ meV for the B state.

5. Concluding Remarks

The present paper deals with the collision energy dependence of the chemiluminescent $Ca^*(^1D_2) + HBr \rightarrow CaBr^*(A,B) + H$ reactions and reports both experimental data and a theoretical study using a dynamical treatment for the nonadiabatic transitions involved in these excited "harpoon" dominated reactions.

From the experimental point of view one aspect of major significance of the present investigation relies on the capability to measure reaction cross-section data for reactions involving both reagent and product electronically excited. In addition an interesting feature of the time-of-flight technique, under crossed-beam conditions, is the energy resolution of the order of $\Delta E \approx$ 15−20 meV. This allowed us to resolve a pronounced maximum (around $E = 215$ meV) followed by a clear post-maximum decline in the reaction cross section of both A and B excited channels, over the 210−290 meV energy range. Whereas the overall shape of both excitation function showed an overall similarity, some oscillations were more noticeable in the reaction cross section for the formation of the B rather than for that leading to the A state.

As far as theory is concerned, our work aimed at developing a model to account for the general features of the observed excitation functions, and no attempt has been made to explain nonmonotonic behavior in the reaction cross-section energy dependence especially observed in the B channel. This will be considered in a forthcoming study.

The interplay between theory and experiments of the present work should be remarked upon. First of all the abrupt maximum in the reaction cross section was attributed to the energy barrier of the inner crossing between the entrance channel of the $Ca^*(^1P_1) + HBr$ and the ionic potential leading to reaction products in the electronically excited states. In addition, the post maximum decline in the excitation function was properly described when the usual Landau−Zener model was modified to incorporate molecular rearrangement of the reaction intermediate. The evidence is presented here for the necessity of synchronization between nonadiabatic transitions and molecular rearrangement. The overall effect produces a limitation of the range of reaction impact parameters: interestingly a reaction window for impact parameters was suggested from the analysis of the internal states of the products in the analogous case of the $Ca^* + HF$ reactions.[17]

The concept of the time scale introduced in the electron jump formalism, necessary to induce molecular rearrangement (therefore, the transition from the entrance neutral to the exit ionic channel) is perhaps one of the most important clues for a proper treatment of dynamics. Certainly, this idea opens new possibilities to study chemical reactions involving electron transfer. This may be relevant for surface hopping calculations. It must be substantiated by exact quantum mechanical calculations, both of the time delay (as the logarithmic derivative of the S matrix) and of its relevance for overall multichannel dynamics.

Acknowledgment. The work in Perugia is supported by the Italian National Researc Council (CNR), by the Ministero dell'Universitá e della Ricerca scientifica (MURST), and by Europian Union through the program Training and Mobility of Researchers Network "Potential Energy Surfaces for Molecular Spectroscopy and Dynamics" [Contract ERB-FMRX-CT96-0088]. The work in Madrid is supported by the DGICYT of Spain under Grant PB95/391.

References and Notes

(1) Brinkmann, U.; Telle, H. *J. Phys. B* **1977**, *77*, 133.
(2) Rettner, C. T.; Zare, R. N. *J. Chem. Phys.* **1982**, *77*, 2416.
(3) Garay, M.; Esteban, M.; Verdasco, E.; González Ureña, A. *Chem. Phys.* **1995**, *195*, 235.
(4) Keller, A.; Lawruszczuk, R.; Soep, B.; Visticot, J. P. *J. Chem. Phys.* **1996**, *105*, 4556. Soep, B.; Whitham, C. J.; Keller, A.; Visticot, J. P. *Faraday Discuss. Chem. Soc.* **1991**, *91*, 191.
(5) Esteban, M.; Garay, M.; García Tejero, J. M.; Verdasco, E.; González Ureña, A. *Chem. Phys. Lett.* **1994**, *230*, 525. Verdasco, E.; González Ureña, A. *J. Chem. Phys.* **1990**, *93*, 428.
(6) Bobashev, S. V.; Kharchenko, V. A. In Electronic and Atomic Collisions, Book of Abstracts XVII; McCarthy, I. E., McGillivray, W. R., Standage, M. C., Eds.; IPEAC: New York, 1991; p 664. 1991; We thank Drs Bobashev and Kharchenko for extensive information and discussion on this formula. For a previous application to an electronic-to-vibrational energy transfer process, see: Aquilanti, V.; Candori, R.; Pirani, F.; Ottinger, Ch. *Chem. Phys.* **1994**, *187*, 171.
(7) Garay, M.; González Ureña, A.; Gareth, R. *Isr. J. Chem.* **1997**, *37*, 353. Menéndez, M.; Garay, M.; Verdasco J. E.; González Ureña, A. *J. Chem. Soc., Faraday Trans.* **1993**, *89*, 1493.
(8) De Castro Vítores, M.; Candori, R.; Pirani, F.; Aquilanti, V.; Menéndez, M.; Garay, M.; González Ureña, A. *J. Phys. Chem.* **1996**, *100*, 7997.
(9) Correlation formulas between potential parameters and polarizabilities of the interacting neutral−neutral partners are given in Cambi, R.; Cappelletti, D.; Liuti, G.; Pirani, F. *J. Chem. Phys.* **1991**, *95*, 1852. Extensions to ion−neutral and ion−ion cases are given respectively in Cappelletti, D.; Liuti; G.; Pirani, F. *Chem. Phys. Lett.* **1991**, *183*, 297, and Aquilanti, V.; Cappelletti, D.; Pirani, F. *Chem. Phys.* **1996**, *209*, 299.
(10) De Castro, M.; Candori, R.; Pirani, F.; Aquilanti, V.; Garay, M.; González Ureña, A. *Chem. Phys. Lett.* **1996**, *263*, 456.
(11) Dubernet, M.-L.; Hutson, J. M. *J. Chem. Phys.* **1994**, *101*, 1939. Dubernet, M.-L.; Hutson, J. M. *J. Phys. Chem.* **1994**, *98*, 5844.
(12) Magee, J. L. *J. Chem. Phys.* **1940**, *8*, 687. For recent extensions and applications, also see: Aquilanti, V.; Cappelletti, D.; Pirani, F. *Chem. Phys. Lett.* **1997**, *271*, 216, and Aquilanti, V.; Cappelletti, D.; Pirani, F. *J. Chem. Phys.* **1997**, *106*, 5043.
(13) Herschbach, D. R. *Adv. Chem. Phys.* **1966**, *10*, 319.
(14) Landau, L. D. *Phys. Z. Sowjetunion* **1932**, *2*, 46.
(15) Zener, C. *Proc. R. Soc.* London **1932**, *A 137*, 696.
(16) Stückelberg, E. C. G. *Helv. Phys. Acta* **1932**, *5*, 369.
(17) Engelke, F.; Meiwes-Broer, K. H. *Chem. Phys. Lett.* **1984**, *108*, 132; in *Selectivity in Chemical Reactions*; Whitehead, J. C., Ed.; Kluwer: New York, 1988; p 135.